Simulated body fluid nucleation of poly(vinyl alcohol)/nanohydroxyapatite hydrogels

Areli M. Salgado-Delgado[1), 2), *)]**, Heriberto Hernández-Cocoletzi**[1)]**, Efrain Rubio-Rosas**[1)]**,
Alejandro Escobedo-Morales**[1)]**, Ernesto Chigo-Anota**[1)]**, Alfredo Olarte-Paredes**[1), 2)]**,
Rene Salgado-Delgado**[2)]**, Victor M. Castaño**[3), **)]

Abstract: Novel poly(vinyl alcohol) (PVA) and chitosan (CS) or 2-hydroxyethyl methacrylate (HEMA) and nanohydroxyapatite (nanoHAp) electrospinning-produced membranes were evaluated, in terms of their bioactivity under exposure to simulated body fluid (SBF). After soaking them in SBF for 5, 8 and 15 days, the scanning electron microscopy (SEM) images show the accumulation of calcium carbonate or calcium phosphate SBF on the surface of the nanohydroxyapatite (nanoHAp). This indicates that there might be an increased bioactivity on the surface of the nanoHAp prepared by this method.

Keywords: simulated body fluid (SBF), biopolymers, bioactivity, electrospinning.

Nukleacja hydrożeli poli(alkohol winylowy)/nanohydroksyapatyt w symulowanym płynie ustrojowym

Streszczenie: Zbadano bioaktywność nowych membran, otrzymywanych w wyniku elektroprzędzenia z hydrożeli poli(alkoholu winylowego) (PVA) z chitozanem (CS), metakrylanem 2-hydroksyetylu (HEMA) i/lub nanohydroksyapatytem (nanoHAp), poddanych działaniu symulowanego płynu ustrojowego (SBF). Metodą skaningowej mikroskopii elektronowej (SEM) stwierdzono, że po zanurzeniu wytworzonych membran w roztworze SBF na 5, 8 i 15 dni na powierzchni cząstek nanoHAp w badanych próbkach nastąpiła akumulacja cząsteczek węglanów i fosforanów wapnia pochodzących z SBF, co dowodzi, że tą metodą można zwiększyć bioaktywność przygotowanych membran, przeznaczonych do zastosowania w rekonstrukcji tkanki kostnej.

Słowa kluczowe: symulowany płyn ustrojowy (SBF), biopolimery, bioaktywność, elektroprzędzenie.

Bone is an essential supportive structure of the body, characterized by its rigidity, hardness, and regeneration ability. It serves to guard necessary organs, produces blood cells, acts as a mineral reservoir for calcium and maintains acid-base balance. Ceramics, natural and synthetic polymers are used in scaffold preparation [1].

Polymers are mostly made out of organic components and are characterized by macromolecular properties comparable to lipids, proteins and polysaccharides, which are key functional organic components of the biological environment. A variety of biodegradable natural and synthetic polymers has also been extensively investigated for biomedical applications [2].

Poly(vinyl alcohol) hydrogel (PVA) is a hydrophilic semicrystalline biodegradable polymer with low toxicity, which presents many excellent properties such as chemical properties stability, availability and low cost of the molding, and well biocompatibility. It has been widely studied as a potential artificial replacement material in previous studies for biomedical and tissue engineering applications [3–7].

2-Hydroxyethyl methacrylate (HEMA) has many applications in medicine and industry. It is known as important substance that is used extensively in a wide range for both industrial and biomedical applications [8]. Because of their biocompatibility, for instance, molecularly engineered hydrogels based on HEMA have been shown to be potential carriers in drug delivery, dental, ophthalmic, and neural tissue engineering applications [9–11].

Chitosan (CS) is a semisynthetic polymer which is generally used alone or in combination with different poly-

[1)] Benemérita Universidad Autónoma de Puebla, Edificio 106H, Ciudad Universitaria, Av. Sn. Claudio y 18 sur, Col. Jardines de San Manuel, Puebla, Puebla, México, C.P. 72570.
[2)] Tecnológico Nacional de México, Instituto Tecnológico de Zacatepec, Calzada Tecnológico núm. 27, Prolongación Plan de Ayala, Zacatepec, Morelos, México, C.P. 62780.
[3)] Centro de Física Aplicada y Tecnología Avanzada, Universidad Nacional Autónoma de México, Boulevard Juriquilla 3001, Querétaro, Querétaro, México, C.P. 76230.
Authors for correspondence;
e-mail: *) amsd_2303@hotmail.com , **) vmcastano@unam.mx

mers or ceramics as scaffolds in bone tissue engineering [12]. Scaffolds are prepared by several techniques such as fiber bonding, melt molding, solvent casting, gas foaming and phase separation [13–18].

Thin membranes make good candidates for membrane scaffold due to their water absorbance and retention characteristics [19]. These polymers can increase their volume several times when exposed to aqueous environments, property that allows water release in a controlled way, preventing possible membrane denaturalization [20, 21]. The preparation and characterization of mimetic functional membranes is a modern and relevant topic in nanomedicine and biotechnology fields [22, 23].

Electrospinning is one of the techniques to prepare scaffolds ranging from nanoscale to microscale fibers, and the nanostructures prepared by this technique resemble the native components of the extracellular matrix [12].

In several bone tissue engineering strategies, bioactive materials in the form of highly porous structures, termed scaffolds, are required [24], and they depend on biomaterials, cell formation capacity, regulatory signals and techniques applied (Fig. 1).
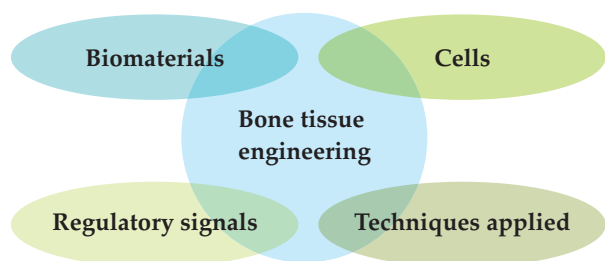

Fig. 1. Bone tissue engineering elements

Two decades ago, Kokubo *et al*. used simulated body fluid (SBF) to perform *in vitro* simulations of *in vivo* conditions. In 2006, Kokubo and Takadama reiterated the statement that SBF could be used to test [25, 26].

SBF has been applied to generate mineralized layer [27]. Immersion in SBF can also be used to measure the ability of biomaterials in formation of apatite layer to predict the bioactivity *in vivo* [28]. This may enhance the bioactivity of ceramics. However, the SBF measurement is considered as an indicator of bioactivity of ceramics because of the differences between the actual *in vivo* process of biomaterial integration inside a living human body and the process of measuring apatite-forming ability of biomaterials inside SBF solution [29]. Therefore, whether SBF treatment on ceramics has the ability to enhance bioactivity [30] or not was uncertain to us.

In this study, the impact of SBF immersion for 5, 8 and 15 days on bioactivity hydrogels based on PVA obtained by electrospinning was investigated. The performance of the surface modified specimen was then evaluated using various surface characterization techniques.

EXPERIMENTAL PART

Materials

In this work we used poly(vinyl alcohol) (PVA) industrial grade, chitosan medium molecular weight (CS, CAS No. 9012-76-4), 2-hydroxyethyl methacrylate (HEMA, CAS No. 868-77-9), hydroxyapatite (nanoHAp, < 200 nm, CAS No. 12167-74-7), acetic acid (CAS No. 64-19-7), glutaraldehyde solution 50 wt % in H_2O (CAS No. 111-30-8), calcium chloride anhydrous 97 % ($CaCl_2$, CAS No. 10043-52-4), sodium chloride (NaCl, CAS No. 7647-14-5), tris(hydroxymethyl)aminomethane 99.8 % [$NH_2C(CH_2OH)_3$, TRIS, CAS No. 77-86-1] and hydrochloric acid 37 % (HCl, CAS No. 7647-01-0) purchased from Sigma Aldrich.

Solution preparation

Chitosan solution (3 % w/v) was prepared in an aqueous 1 % v/v acetic acid solution. PVA solution was prepared by dissolving PVA in 3 : 2 alcohol : water solution under mechanical stirring for 1.5 h at 60 °C. PVA composite solutions were prepared using analogous procedures, adding CS, HEMA and nanoHAp as mentioned in Table 1.

T a b l e 1. Matrix of composite solutions

Sample	PVA g	CS (3 % w/v) cm³	HEMA cm³	nanoHAp mg
PVA	8			
PVA/CS	8	1		
PVA/nanoHAp	8	1		5, 10, 15
PVA/HEMA/nanoHAp	8		0.3	5, 15

Electrospinning setup

The experimental setup used for electrospinning process consists of a high-voltage power supply (0–40 kV), a plastic syringe containing the polymer solution and syringe needles with an internal diameter of about 0.5 mm, as can be observe in Fig. 2.

The electrospinning exposition was carried for 60 min and 25 kV.

The composite fibers were collected by a rotational collector which rotates at a constant speed (200 rpm). The negative electrode was connected to the collector and the positive electrode was connected to a needle. Considering the described scaffold materials, several types of tubular scaffolds are proposed and investigated in this study. The choice of the scaffold concepts was based on tissue development.

Solutions for *in vitro* tests

In this study, the behavior of the scaffold was investigated by exposing the materials in simulated body fluid
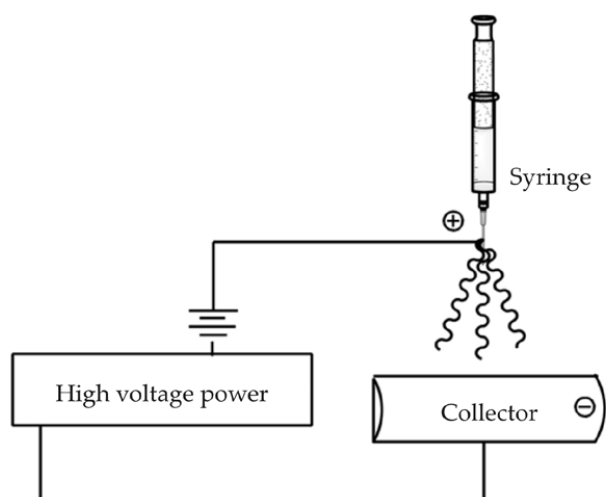
Fig. 2. Schematic of electrospinning setup

(SBF), according to the Kokubo methodology taking into account the variations in concentration in SBF. The pH value was set at 7.38–7.44 at 36 °C. The ion composition of SBF solution is shown in Table 2. The SBF solution was refreshed every 8 days to maintain the ion concentration that decreased due to calcium and phosphorous deposition on the samples [31].

T a b l e 2. **Composition of simulated body fluid (SBF)**

Volume	1000 cm³	500 cm³	250 cm³
Concentration	1.5 M	1.5 M	1.5 M
$CaCl_2$	0.249 g	0.1245 g	0.06225 g
K_2HPO_4	0.255 g	0.1175 g	0.05875 g
NaCl	12.535 g	6.2675 g	3.13375 g
TRIS	6.055 g	3.0275 g	1.51375 g

Methods of testing

– The morphology and microstructure of the samples were evaluated using scanning electron microscopy

(SEM). The electrospinning fiber samples were coated with a thin layer of gold by sputtering (Denton Vacuum, model Desk V) and their morphologies were observed under a scanning electron microscope JEOL model JSM-6810LV that operated at voltage of 20 kV. The apatite growth was observed.

– The samples were examined by Fourier transform infrared (FT-IR) analysis with a PerkinElmer model Spectrum Two, at room temperature (27 °C). The samples were analyzed with 16 scans averaging 4 cm⁻¹ resolution between 4000 cm⁻¹ to 650 cm⁻¹. The FT-IR analysis was used to characterize the presence of specific chemical groups of apatite.

RESULTS AND DISCUSSION

The *in vitro* bioactivity of samples of composite hydrogels based on PVA and nanoHAp was assessed by immersion in an SBF solution. Sample modifications were evaluated by SEM analysis. SEM analysis confirmed that after the immersion in SBF solution, the samples didn't preserved their fibrillar structure, SEM examination also showed that in case of the surface of all samples covered by a mineral, it was possible to observe the presence of apatite growth on the surface which was greater for samples containing nanoHAp, since the presence of nanoHAp in the material increases the nucleation points for the apatite.

In Fig. 3, it is observed that in the PVA the fiber structure was lost in the membrane, evidencing that after 8 days of immersion in SBF there was a growth of apatite on the PVA surface: mineral crystals covered most regions of the surface of the samples, but the mineral layer formed was very thin and the PVA could still be seen.

In case of the PVA/CS membrane it was observed (Fig. 4) that the apatite growth on its surface was carried out with 5 days of immersion in SBF, increasing this formation in 8 (Fig. 4c) and 15 days of immersion (Fig. 4d).

With the addition of nanoHAp in the composites based on PVA, it was observed that the apatite growth was more evident, due the nucleation points increased with the
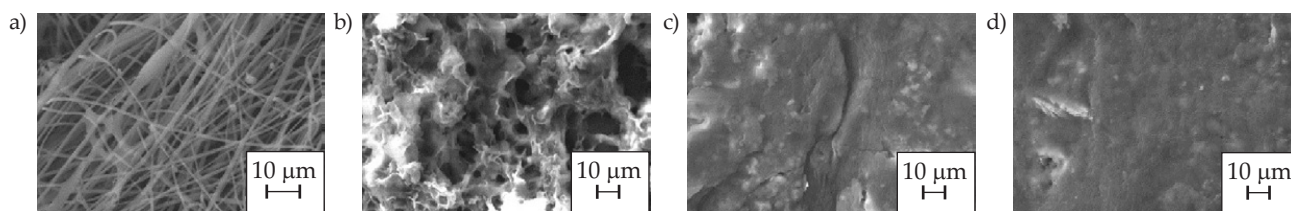

Fig. 3. SEM of PVA: a) before SBF (1500×), b) after 5 days SBF (1000×), c) after 8 days SBF (1000×), d) after 15 days SBF (1000×)
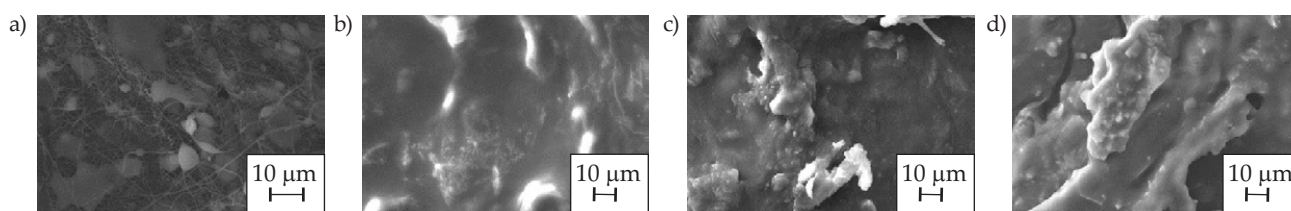

Fig. 4. SEM of PVA/CS: a) before SBF (1500×), b) after 5 days SBF (1000×), c) after 8 days SBF (1000×), d) after 15 days SBF (1000×)
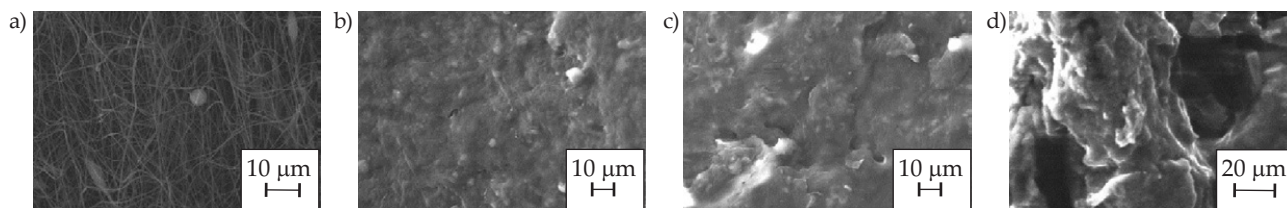
Fig. 5. SEM PVA/nanoHAp 5 mg: a) before SBF (1500×), b) after 5 days SBF (1000×), c) after 8 days SBF (1000×), d) after 15 days SBF (1000×)
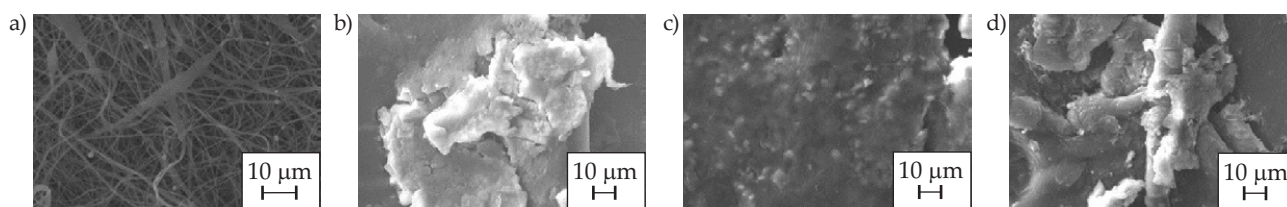

Fig. 6. SEM of PVA/nanoHAp 10 mg: a) before SBF (1500×), b) after 5 days SBF (1000×), c) after 8 days SBF (1000×), d) after 15 days SBF (1000×)
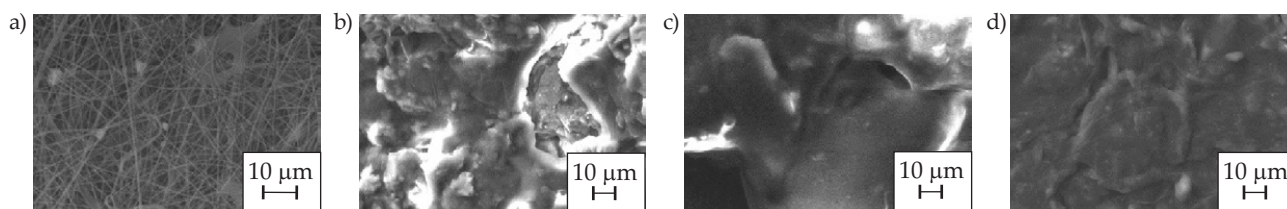

Fig. 7. SEM of PVA/nanoHAp 15 mg: a) before SBF (1500×), b) after 5 days SBF (1000×), c) after 8 days SBF (1000×), d) after 15 days SBF (1000×)
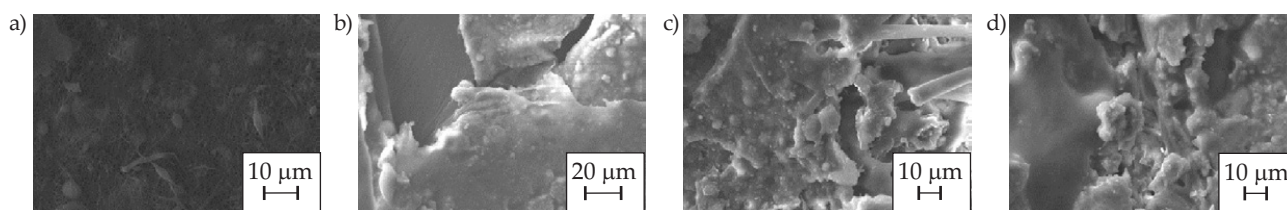

Fig. 8. SEM of PVA/HEMA/nanoHAp 10 mg: a) before SBF (1500×), b) after 5 days SBF (800×), c) after 8 days SBF (1000×), d) after 15 days SBF (1000×)
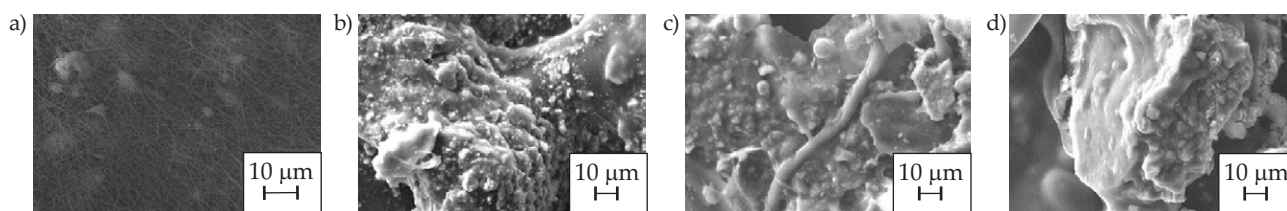

Fig. 9. SEM of PVA/HEMA/nanoHAp 15 mg: a) before SBF (1500×), b) after 5 days SBF (1000×), c) after 8 days SBF (1000×), d) after 15 days SBF (1000×)

presence of nanoHAp, having an acceptable bioactivity in the samples (Fig. 5). The bioactivity in the samples increases with increasing of the ceramic's concentration of 5, 10 and 15 mg (Figs. 5, 6 and 7) as a function of both the concentration and the days of immersion in SBF.

In the case of PVA/HEMA/nanoHAp membranes, the structure of the fibers is no longer observed as before the immersion in SBF, but the growth of apatite on the surface of the membrane is more evident as a function of the nanoHAp concentration increased (10 and 15 mg) and

the SBF immersion time (5, 8 and 15 days), as seen in the Figs. 8 and 9.

The FT-IR spectra of the mineralized PVA/HEMA/nanoHAp membranes are shown in Fig. 10.

The absorption peaks of PVA were observed at 1464 cm^{-1} (bending of OH and wagging of CH_2), 1374 cm^{-1} (stretching of C=O), and 1092 cm^{-1} (stretching of CO and bending of OH from amorphous sequence of PVA). The peak on 1142 cm^{-1} increased after the SBF immersion, the intensity of this peak is influenced by the
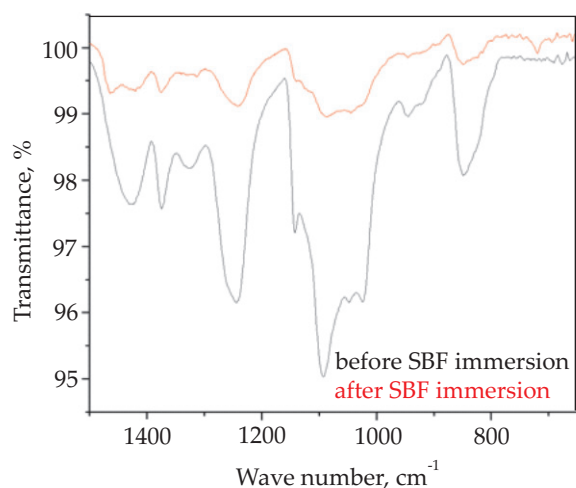
Fig. 10. FT-IR analysis of PVA/HEMA/nanoHAp before and after SBF immersion

crystalline portion of the apatite growth. On the other hand, the formation of apatite is evidenced by P–O asymmetric stretching bands lying at 1000–1144 and at 946 cm^{-1} corresponding to PO_4^{-3} group of nanoHAp. However, there are also vibrational bands corresponding to the carbonate groups [CO_3^{2-}] (840, 1430 cm^{-1}) after immersion in SBF due to the organic origin that has the apatite.

CONCLUSIONS

The formation of apatite active layer occurs within a short period on the surface of the PVA and nanoHAp composites obtained by electrospinning technique after soaking in SBF. It demonstrates high *in vitro* bioactivity of tested samples and makes the composite suitable candidate for applications in tissue engineering. In case of the addition of HEMA and 15 mg nanoHAp after 5 days of immersion, this behavior is more evident, showing excellent bioactivity. The bioactivity property of the composite under exposure to SBF solution can be tailored by varying the nanoHAp concentration in the composite [32]. The FT-IR analysis showed the increase of apatite after the SBF immersion.

REFERENCES

[1] Gang W., Su B., Zhang W., Wang C.: *Materials Chemistry and Physics* **2008**, *107*, 364.
http://dx.doi.org/10.1016/j.matchemphys.2007.07.028
[2] "Biomedical Foams for Tissue Engineering Applications" 1st Edition (Ed. Netti P.), Woodhead Publishing, 2017.
[3] Trieu H., Qutubuddin S.: *Polymer* **1995**, *36* (*13*), 2531.
http://dx.doi.org/10.1016/0032-3861(95)91198-g
[4] Brostow W., Hagg Lobland H.E.: "Materials: Introduction and Applications", John Wiley & Sons, 2017.
[5] Brostow W., Kumar P., Vrsaljko D., Whitworth J.: *Journal of Nanoscience and Nanotechnology* **2011**, *11*, 3922.
https://doi.org/10.1166/jnn.2011.3849
[6] Freeman M., Furey M., Love B., Hampton J.: *Wear* **2000**, *241*, 129.
http://dx.doi.org/10.1016/s0043-1648(00)00387-2
[7] Pan Y., Xiong D., Ma R.: *Wear* **2007**, *262*, 1021.
http://dx.doi.org/10.1016/j.wear.2006.10.005
[8] Abbaszadeh F., Moradi O., Norouzi M., Sabzevari O.: *Journal of Industrial and Engineering Chemistry* **2014**, *20*, 2895.
http://dx.doi.org/10.1016/j.jiec.2013.11.025
[9] Stamatialis D., Papenburg B., Gironés M. *et al.*: *Journal of Membrane Science* **2008**, *308*, 1.
http://dx.doi.org/10.1016/j.memsci.2007.09.059
[10] Hung C., Kuo C., Weng N. *et al.*: *Polymer Journal* **2016**, *48*, 439.
http://dx.doi.org/10.1038/pj.2015.127
[11] Barve R., Chaughule R.: *Journal of Nanostructure in Chemistry* **2013**, *3* (*1*), 18.
http://dx.doi.org/10.1186/2193-8865-3-18
[12] Balagangadharan K., Dhivya S., Selvamurugan N.: *International Journal of Biological Macromolecules* **2017**, *104*, 1372.
https://doi.org/10.1016/j.ijbiomac.2016.12.046
[13] Swetha M., Sahithi K., Moorthi A. *et al.*: *International Journal of Biological Macromolecules* **2010**, *47*, 1.
http://dx.doi.org/10.1016/j.ijbiomac.2010.03.015
[14] Sainitya R., Sriram M., Kalyanaraman V. *et al.*: *International Journal of Biological Macromolecules* **2015**, *80*, 481.
http://dx.doi.org/10.1016/j.ijbiomac.2015.07.016
[15] Dhivya S., Saravanan S., Sastry T., Selvamurugan N.: *Journal of Nanobiotechnology* **2015**, *13*, 40.
http://dx.doi.org/10.1186/s12951-015-0099-z
[16] Raz M., Moztarzadeh F., Kordestani S.: *Silicon* **2018**, *10*, 277.
http://dx.doi.org/10.1007/s12633-016-9439-3
[17] Venkatesan J., Bhatnagar I., Kim S.: *Marine Drugs* **2014**, *12*, 300.
http://dx.doi.org/10.3390/md12010300
[18] Tripathi A., Saravanan S., Pattnaik S. *et al.*: *International Journal of Biological Macromolecules* **2012**, *50*, 294.
http://dx.doi.org/10.1016/j.ijbiomac.2011.11.013
[19] González-Henríquez C., Sarabia-Vallejos M.: *Chemistry and Physics of Lipids* **2015**, *190*, 51.
http://dx.doi.org/10.1016/j.chemphyslip.2015.07.004
[20] Ross E., Mok S., Bugni S.: *Langmuir* **2011**, *27*, 8634.
http://dx.doi.org/10.1021/la200952c
[21] Roerdink Lander M., Ibragimova S., Rein C. *et al.*: *Langmuir* **2011**, *27*, 7002.
http://dx.doi.org/10.1021/la1050699
[22] Zhang W., Sun J., Liu Y. *et al.*: *Molecular Pharmaceutics* **2014**, *11*, 3279.

http://dx.doi.org/10.1021/mp400566a

[23] Mikkola S., Robciuc A., Lokajová J. *et al.*: *Environmental Science* & *Technology* **2015**, *49*, 1870.
http://dx.doi.org/10.1021/es505725g

[24] Rohanová D., Boccaccini A., Yunos D. *et al.*: *Acta Biomaterialia* **2011**, *7* (*6*), 2623.
http://dx.doi.org/10.1016/j.actbio.2011.02.028

[25] Kokubo T., Takadama H.: *Biomaterials* **2006**, *27*, 2907.
http://dx.doi.org/10.1016/j.biomaterials.2006.01.017

[26] Sooksaen P., Chaithep K., Saliwong T., Duangart T.: *Advanced Materials Research* **2012**, *506*, 146.
http://dx.doi.org/10.4028/www.scientific.net/amr.506.146

[27] Huang L., Zhou B., Wu H. *et al.*: *Materials Science and Engineering: C* **2017**, *70*, 955.
http://dx.doi.org/10.1016/j.msec.2016.05.115

[28] Kawai T., Takemoto M., Fujibayashi S. *et al.*: *Journal of Biomedical Materials Research Part B: Applied Biomaterials* **2014**, *103*, 1069.
http://dx.doi.org/10.1002/jbm.b.33281

[29] Zadpoor A.: *Materials Science and Engineering: C* **2014**, *35*, 134.
http://dx.doi.org/10.1016/j.msec.2013.10.026

[30] Wang K., Leng Y., Lu X. *et al.*: *CrystEngComm* **2012**, *14* (*18*), 5870.
http://dx.doi.org/10.1039/c2ce25216c

[31] Wang M., Li Y., Wu J. *et al.*: *Journal of Biomedical Materials Research Part A* **2008**, *85A* (*2*), 418.
http://dx.doi.org/10.1002/jbm.a.31585

[32] Bustos-Ramírez K., Martínez-Hernández A.L., Martínez-Barrera G. *et al.*: *Materials* **2013**, *6* (*3*), 911.
http://dx.doi.org/10.3390/ma6030911